ASTRONOMY & ASTROPHYSICS
SUPPLEMENT SERIES

Astron. Astrophys. Suppl. Ser. **51**, 365-384 (1983)

Spectrophotometry of peculiar B and A stars. XIII. HD 51418, 53 Camelopardalis, 78 Virginis, and Kappa Piscium

D. M. Pyper (*), (**)

Department of Physics, University of Nevada, Las Vegas, NV 89154, U.S.A.

and S. J. Adelman (**)

Department of Physics, The Citadel, Charleston, SC 29409, U.S.A.

Received July 26, accepted September 22, 1982

Summary. — Optical region spectrophotometry of four Ap stars having moderate to cool temperatures shows that the λ 4200 and λ 5200 broad absorption features are strong in all four stars. Except for a slight variability of the λ 5200 feature in HD 51418, there is no convincing evidence for variation of these features with phase in any of the stars. The strength of the broad absorption features is not strongly correlated with the slope of the red end of the Paschen continuum or with the apparent amount of differential absorption present in the shortward end of the Paschen continuum. The star HD 51418 is an outstanding spectrum and photometric variable but shows weak or no variations of the broad absorption features. Further study of this and several similar stars should help clarify the origin of the broad absorption features.

Key words : peculiar A Stars — spectrophotometry — broad absorption features — line blanketing.

1. **Introduction.** — In this paper we present optical region spectrophotometry for four Ap spectrum variables, HD 51418, 53 Cam, 78 Vir and κ Psc, which have moderate to cool temperatures for this type of star. Both 53 Cam and HD 51418 exhibit large spectrum variations, while 78 Vir and κ Psc do not. Table I summarizes the spectrum, photometric and magnetic data available at present on these four stars, plus the values of i estimated on the basis of rigid rotator models. For this small sample of stars it appears as though the spectrum and photometric variations are correlated with each other and with the estimated values of i, while the magnetic field variations display a weaker correlation. This is not always the case for magnetic Ap stars ; some stars (e.g., HD 215441) show strong photometric variations but the spectrum variations are weak in the optical region.

The data reduction techniques, and those for forming the various indices, have been discussed in paper I (Adelman, 1979), paper III (Adelman and Pyper, 1979), and paper IV (White *et al.*, 1980) of this series. A recalibration of the indices is discussed in the appendix. The stars considered here have optical flux envelopes that show major deviations from those of normal main sequence stars in the shortward part of the Paschen continuum.

Table II contains the Journal of Observations for all four stars, table III summarizes the four-color photometry in the literature compared with that of D. M. P. in this paper and the *u-b* and *b-y* colors synthesized from our spectrophotometry, and table IV lists the temperatures obtained by various authors compared to those determined from our data. Table V gives the photometric results of D. M. P. for HD 51418,53 Cam and κ Psc, and tables VI-IX give the energy distributions and synthesized indices for HD 51418, 53 Cam, 78 Vir and κ Psc, respectively. The model atmospheres used for comparison with the Ap star energy distributions are in all cases solar composition, $\log g = 4.0$ models of Kurucz (1979). The theoretical colors based on model atmospheres were calculated by Relyea and Kurucz (1978).

2. **HD 51418.** — HD 51418 is an Ap spectrum variable with the iron peak elements and the REE varying in phase with each other and with Sr II about 180° out of phase with them (Gulliver, 1972; Gulliver and Winzer, 1973). Jones *et al.* (1974) found that the maximum $H_{\rm eff}$ is at REE and iron peak maximum and that the heavier REE, especially H_o, are apparently more enhanced than are the lighter REE such as Ce and Sm. Hardorp (1976) found $v \sin i$ to be 18 km.s^{-1}.

The *UBV* photometry of HD 51418 by Gulliver and

(*) Guest Investigator, Mt. Wilson Observatory of the Carnegie Institution of Washington.

(**) Visiting Astronomer, Kitt Peak National Observatory, which is operated by the Association of Universities for Research in Astronomy, Inc., under contract with the National Science Foundation.

Send offprint requests to : D. M. Pyper Smith.

Winzer (1973) showed that this star is a large amplitude single wave light variable. Their ephemeris is

$$\text{JD(maximum } V) = 2441241.654 + 5.4379\,E\,.$$

The *B-V* and *U-B* colors are bluest near minimum *V*, while the Hβ index varies out of phase with the REE and iron peak elements. Photometric *uvby* observations were made by D. M. P. from 1979-81 with the # 4 40-cm telescope at Kitt Peak National Observatory. The data are presented in tables III and V. The comparison star, 60 Aur, was also used by Gulliver and Winzer. Previously published values of *b-y* and *u-b* by Cameron (Table III) differ by 2 σ or more from the values measured by D. M. P. Reductions were made following Crawford and Barnes (1970) and Crawford and Mander (1966) with modified versions of K.P.N.O computer programs. The Δy (HD 51418 − 60 Aur) observations of D. M. P. agree both in amplitude and phase (Fig. 1) with the ΔV values of Gulliver and Winzer. Not enough *uvby* or Hβ data are now available to refine the period of HD 51418.

The *b-y* and *u-b* colors synthesized from the spectrophotometry, when plotted *vs.* phase (Fig. 2), agree well with the *b-y* and *u-b* curves obtained by D. M. P. Of the other indices, also plotted *vs.* phase in figure 2, the Δa values of scans 1-3 are systematically lower than those of scans 4-15, probably due to sparser wavelength coverage in the former group of scans. The values of scans 4-15 suggest that Δa is variable (amplitude $\cong 0^{m}.02$) with its minimum near $\phi = 0.5$, and the λ 4200 indices, especially $\Delta\imath$**, may be larger at about the same phase. However, the variability of the shortward end of the Paschen continuum combined with the small values of the λ 4200 indices make it difficult to interpret these data. Inspection of the average energy distribution and the average index values (Table VI, Fig. 3) indicate the presence of weak and moderately strong λ 4200 and λ 5200 continuum absorption features, respectively. The λ 5200 feature was previously discovered in HD 51418 by Hardorp (1976). Our data shows it to have a sharp core and broad wings but it does not have as much structure as is seen in the cooler Ap star 53 Cam (Sect. 3). Figure 4 shows averages at the two phases of maximum difference in *b-y* ($\phi = 0.45$ and 0.0) to illustrate the large changes in the energy distribution over the cycle of variation. The data is normalized to λ 4032, the region where the photometric variability has the smallest amplitude (Fig. 1). This is the only star observed by us so far that shows behavior of this magnitude and nature. There is also a change in the slope of the Balmer continuum as well as in the longward part of the λ 5200 feature. The longward part of the Paschen continuum ($\lambda \gtrsim 6000$ Å) does not show a change in slope. From $\phi = 0.8$ to 0.1, the λ 4200 feature shows a sharp core. This cannot be due to the spectrum variations of λ 4215 Sr II, since the Sr II line strength is at a minimum at these phases (Gulliver and Winzer, 1973). The λ 6370 and λ 6440 magnitudes are below those of the surrounding wavelengths, which may indicate that a weak λ 6300 absorption feature is present.

Our average value of *u-b* matches that of a 10425 K model atmosphere. The energy distribution of HD 51418 does not match the predictions of any of the model atmospheres tried by us. The best fit to the Paschen continuum longward of 5700 Å is a 9000 K model. There is a large depression of the continuum from 4000-4500 Å and the best fit to the Balmer jump is a 11500 K model. However, the slope of the 9000 K model fits the Balmer continuum better (Fig. 3). There is probably flux redistribution from the far ultraviolet here as in other Ap stars studied so far. Apparently a large amount of variable line blanketing is present, with the blue-violet magnitudes being depressed the most at $\phi = 0.0$ when the REE and iron peak line strengths are at a maximum (Fig. 4). The four-color curves of D. M. P. (Fig. 1) show a maximum amplitude of variation for *y* ($\sim 0^{m}.2$) and a minimum for *v* ($\sim 0^{m}.04$), while *b* and *u* vary with an amplitude of about $0^{m}.1$; all magnitudes vary in phase. Our spectrophotometry yields similar results for the three nights ($\phi = 0.05$, 0.17 and 0.43) on which 60 Aur was also observed; the λ 5556, λ 4566, λ 4167 and λ 3509 magnitudes agree in amplitude and phase with the *y*, *b*, *v* and *u* curves, respectively (Fig. 1). This behavior is consistent with flux redistribution from the far ultraviolet (see, e.g., Peterson, 1970 and Wolff and Wolff, 1971), since the maximum brightness in all colors occurs at REE and iron peak maximum absorption. The small amplitude variation of *v* cannot be attributed to variations of Hγ cancelling out the effects of ultraviolet flux redistribution. A spectrophotometric index to measure the strength of Hβ,

$$hb = m(4861) - 0.5[m(4785) + m(4935)]\,,$$

was computed for scans 5-15; *hb* varies with the β values measured by Gulliver and Winzer (1973) and D. M. P. (Fig. 1). Inspection of the scans shows that Hγ varies in the same way as does Hβ, the maximum strength being at $\phi \cong 0.5$. Any changes in Hγ should thus result in *v* being slightly fainter at phase 0.5, which is in phase with the variations of *y*, *b* and *u*. The cause of the small amplitude variation in the violet is probably large variable line blanketing effects due to the REE and iron peak elements, which mask the effects of flux redistribution from the far ultraviolet. Similar effects have been observed in several other Ap stars (Wolff and Wolff, 1971; Maitzen *et al.*, 1978; Hensberge *et al.*, 1981).

3. **53 Cam.** — The SrCrEu Ap star 53 Cam (=HR 3109 =HD 65339) is a spectrum variable with a large reversing magnetic field (Babcock, 1958). The Ca II lines vary out of phase with lines of the iron peak elements and Eu II (Faraggiana, 1973). Photometry by D. M. P. (see Sect. 2) indicates that the β index also varies in phase with the iron peak group, the maxima of both occurring at $H_{\rm eff}$ minimum (Table V, Fig. 5). 53 Cam is a single-lined spectroscopic binary with a period of 2380 days and a high eccentricity orbit (Faraggiana, 1973; Scholz, 1978). Scholz suggests that tidal action may be present near periastron, where the separation of the two components is about 1 AU.

Preston and Stepien (1968) determined a period of $8^{d}.0278$ from photometric and magnetic observations of 53 Cam. A slightly shorter period based on magnetic measurements was determined by Borra and Landstreet (1977) with the ephemeris

$$\text{JD(Positive crossover)} = 2435855.652 + 8.0267\,E\,.$$

This latter period best fits the *uvby* photometry of Wolff and Wolff (1971) and D. M. P. (Fig. 5).

Wolff and Wolff found that *u* and *v* vary in phase but *b* and *y* are 180° out of phase with them. Both the *y* of Wolff and Wolff and the *V* of Preston and Stepien have maxima within 0.1 cycle of the $H_{\rm eff}$ minimum at $\phi = 0.8$. The *b-y* color displays little variation, while *u-b* varies with an amplitude of about 0$^{\rm m}$.05, being bluest at $H_{\rm eff}$ maximum ($\phi = 0.3$). The four-color photometry of D. M. P. (Tables III and V, Fig. 5) confirms this behavior.

Preston (1970) found $v \sin i = 20\ {\rm km\,s^{-1}}$. At $\phi = 0.88$, partially resolved Zeeman patterns yielded a surface magnetic field (H_s) of about − 15 kG (Preston, 1969a). Several investigators (Huchra, 1972; Borra and Landstreet, 1977; Hensberge *et al.*, 1979) have constructed rigid rotator models for 53 Cam, based on measurements of $H_{\rm eff}$ and H_s. All found similar displaced dipole models, summarized in table I.

Our spectrophotometry was carried out at Mt. Wilson Observatory and K.P.N.O. in 1972-74 and at K.P.N.O. in 1978. When compared to the four-color photometry (Table III), our average synthesized *u-b* color is about the same but our *b-y* color is about 0$^{\rm m}$.02 bluer than the other values. Our indices *vs.* phase are plotted in figure 5. It is seen that there is no strong evidence for variation with phase of either *b-y* or *u-b*, with the latter showing a large scatter. In the case of *b-y*, except for the systematic difference, this agrees with the four-color results. However, our *u-b* plot is quite different from the photometric results of D. M. P. The systematic differences seen in figure 5 are probably due to inadequate wavelength coverage in some of our scans and to the irregularity of the spectra of cool Ap stars such as 53 Cam, particularly in the Balmer continuum, which can cause significant changes in $m(\lambda)$ for a slight change in the central wavelength of a bandpass. It should be noted that scans 11, 12 and 13, which have a more extensive wavelength coverage, have synthesized *b-y* and *u-b* values closer to the photometric values. In spite of the systematic difference, the *u-b* values for scans 8, 9 and 10, which are all in the same cycle (connected by a dashed line in Fig. 5), decrease at the same rate as do those of the photometric curve. An examination of these scans shows that the reddening of *u-b* is mainly due to the ultraviolet ($\lambda < 3700$ Å) magnitudes becoming fainter. The four-color results of Wolff and Wolff (1971) were not plotted in figure 5, as they did not publish a journal of observations. As seen in table III, their *b-y* values are the same as those of D. M. P. and their *u-b* values are about 0$^{\rm m}$.01 bluer. This systematic difference may be due to differences in atmospheric transmission between Kitt Peak and Mauna Loa. A similar discrepancy exists for 78 Vir between the *u-b* values of Wolff and Wolff and those of Strömgren and Perry (Table III).

Hardorp (1976) previously reported the presence of the λ 5200 broad continuum feature in 53 Cam. Our average values for the λ 4200 and λ 5200 indices (Table VII) indicate that these two features are strong in this star, which is confirmed by inspection of the average energy distribution in figure 3. Both features display sharp cores and broad wings. The wings of the λ 5200 feature show apparent secondary minima near 5000 and 5556 Å. This was also seen by Adelman (1981a) in stars of similar or cooler temperatures, e.g., HD 5797. The 6370 Å magnitude is fainter than those of the surrounding wavelengths, which may indicate that a weak λ 6300 feature is present, or may be due to differential blanketing. Figure 5 shows no convincing evidence for a phase variation for either the λ 4200 or the λ 5200 feature. Thus they do not show variability which strongly correlates with the strong reversing magnetic field or with the spectrum variations of 53 Cam.

When our average energy distribution is compared to model atmospheres, the predictions of the 8500 K model best fit the Paschen continuum longward of about 5700 Å, but the magnitudes in the range 4000-4700 Å are depressed below those of the model and the Balmer continuum magnitudes are brighter than those of the model (Fig. 3). The Balmer jump can be matched approximately by that of a 10250 K model. However, the slope of the Balmer continuum better matches that of the 8500 K model. Again, the results indicate that we are seeing a flux redistribution from the far ultraviolet, probably complicated by differential line blanketing, which is especially large in the blue-violet.

4. **78 Vir.** — 78 Vir (=HR 5105=HD 118022) was the first star besides the sun in which a magnetic field was detected (Babcock, 1947). Morgan (1932) and Deutsch (1947) studied the spectrum variability of this SrCrEu Ap star, with Ca II, Cr II and Sr II being the principal ions involved. Preston (1969b) determined the periodicity of the magnetic field using his own and Babcock's (1958) data; he found the ephemeris to be

$$\mathrm{JD}(H_{\rm eff}\ \text{maximum}) = 2434816.9 + 3.7220\,E.$$

This period also fits the *UBV* photometry of Stepien (1968), and Winzer (1974), the *VBLUW* photometry of van Genderen (1971) and the *uvby* photometry of Wolff and Wolff (1971).

The photometric studies all show similar results. For example, Wolff and Wolff find that *u*, *v*, *b* and *y* vary in phase with minimum brightness occurring at $H_{\rm eff}$ maximum; *u* has the largest amplitude of about 0$^{\rm m}$.03, and *b-y* and *u-b* show very little variation with phase. The star is seen almost pole on, since it has a relatively short period and $v \sin i$ is only $10\ {\rm km\,s^{-1}}$ (Abt *et al.*, 1972). Borra and Landstreet (1980) find $i = 22°$.

Our spectrophotometry was carried out at Mt. Wilson Observatory and K.P.N.O. in 1972 and at K.P.N.O. in 1976-77. The agreement of our average synthesized *u-b* color with the published values (Table III) is generally good, except that the value of Wolff and Wolff is bluer by about 0$^{\rm m}$.03. Our average value of *b-y* is bluer than any of the published values by at least 0$^{\rm m}$.02.

Our average values for the λ 4200 and λ 5200 indices (Table VIII) indicate that the λ 4200 feature has weak to moderate strength and the λ 5200 feature is moderately strong, which is borne out by inspection of the average energy distribution in figure 3. The λ 5200 feature appears to display some structure, having a sharp core and broad wings. The depression at λ 4200 is apparent, even though the entire spectrum appears to be depressed shortward of about 4700 Å. The 6220 and 6370 Å magnitudes may be slightly depressed, implying the presence of a very weak λ 6300 feature in 78 Vir. The 3509 Å magnitude

also appears bright relative to surrounding wavelengths in all but one of our scans. Maitzen (private communication), from his photometric measurements, finds a small but definite variation in Δa for 78 Vir with a maximum at maximum y. There is no evidence for variation with phase of any of our indices for the λ 4200 and λ 5200 features (Fig. 6). There is large scatter present in the plots of $\Delta a'$ and $\Delta\iota$**, which reflects the large amount of line blanketing in the regions concerned. Slight shifts in the bandpass center wavelengths may cause moderate changes in magnitudes and would introduce more scatter than for a hotter Ap star. There also are systematic differences in b-y and u-b between scans 1-8 and 9-14, apparently due to differences in wavelength coverage (Table VIII, Fig. 6). This will also affect the values of the other indices, which are functions of b-y.

Our average value of u-b corresponds to that of a 9600 K model atmosphere (Table IV). Our average energy distribution cannot be fit by any one atmosphere model; the Paschen continuum is best fit by a 9500 K model, which also fits the wavelengths shortward of 3700 Å reasonably well (Fig. 3). However, the Balmer jump is best fit by a 10000 K model. It is difficult to separate the effect of differential line blanketing from that of flux redistribution in the cooler Ap stars (see also Sect. 4). However, there must be considerable flux redistribution in the spectrum of 78 Vir, since van Dijk *et al.* (1978) have measured a moderately large ultraviolet flux deficiency for this star.

5. **κ Psc.** — The cool Ap star κ Psc (= HR 8911 = HD 220825) is a photometric variable with a short period. Van Genderen (1971) gives an ephemeris of

$$\mathrm{JD0} = 2437198.48 + 0.5853\,E,$$

based on *VBLUW* photometry, but the period is not well determined due to inadequate phase coverage, since earlier photometry by Rakos (1962) was made relative to a variable comparison star. Four-color photometry by D. M. P. (Tables III and V, Fig. 7) is not extensive enough to improve the period, due to the small amplitude of the variations. However, a slightly shorter period ($0^{d}.58525$?) is suggested on comparison of the present data with those of van Genderen. The 0.58-day period, combined with the $v \sin i$ of 38 km . s^{-1} (Abt *et al.*, 1972), implies an almost pole-on orientation of this star (see Table I). Babcock (1958) describes the spectrum as weakly variable (Ca II, Sr II and possibly Eu II). Borra and Landstreet (1980) attempted to measure a magnetic field, but found their values to be less than the errors of measurement in all but one case.

Our spectrophotometry was carried out at Mt. Wilson Observatory in 1972 and at K.P.N.O. in 1972 and 1976 (Table II). Our average synthesized b-y and u-b indices are in fair agreement with previous photometry (Table III) although the u-b values of Strömgren and Perry (1965) and of D. M. P. are $\sim 0^{m}.03$ bluer and the b-y value of Cameron (1966) is $\sim 0^{m}.01$ redder compared to our range of values. The synthesized b-y values when plotted *vs.* phase (Fig. 7) agree with the photometric values of D. M. P. in showing no systematic variation, which is consistent with the low amplitude of variation found in the photometry and the uncertainty in the period. The photometric u-b values of D. M. P. show evidence for a small amplitude variation with a possible minimum near $\phi = 0.5$. The synthesized u-b values are systematically bluer by $\sim 0^{m}.03$. There are not enough synthesized values of u-b to show evidence of variation, due to instrumental problems experienced at Mt. Wilson (see Paper IV). None of the indices Δa, $\Delta a'$ or $\Delta\iota$** show evidence of variation with phase. Maitzen's (private communication) photometric values of Δa for κ Psc also show no clear evidence of variation; he obtains $\Delta a = 0^{m}.032 \pm 0^{m}.003$, for 13 observations.

The average values of the λ 4200 and λ 5200 indices (Table IX) imply the presence of moderate strength λ 4200 and λ 5200 broad continuum features, which is confirmed by examination of the average energy distribution in figure 3. The energy distribution is seen to be quite similar to that of 78 Vir except that κ Psc has a less prominant λ 5200 feature (Fig. 8) and slightly smaller Balmer jump. As is the case for 78 Vir, the red end of the Paschen continuum of κ Psc is closely matched by a 9500 K model atmosphere. However, temperatures estimated by various means are inconsistent (Table IV), the u-b corresponding to $T = 9800$ K and the Balmer jump to $T = 10250$ K. This is due to the abnormal energy distribution, which is probably partly caused by flux redistribution from the far ultraviolet and partly by differential absorption in the blue-violet region of the spectrum.

6. **Discussion.** — In HD 51418, the Δa index shows a variation of amplitude $0^{m}.02$, with a minimum at approximately $\phi = 0.5$ and a maximum at $\phi = 0.0$ (Fig. 2). This is in phase with Δy (maximum at $\phi = 0.0$) and the intensity variations of the REE and Fe peak group. These results imply a 50 % variation in the strength of the λ 5200 feature over the cycle of variation. However, it is not clear whether these variations are due to changes in the feature itself or to changes in the energy distribution outside the feature (i.e., one wing of the feature may change relative to the other). The $\Delta\iota$* and $\Delta\iota$** indices also show a possible variation which is 180° out of phase with that of Δa. This is probably due to the change of slope in the « continuum » between 4000 and 4500 Å. As was mentioned in section 2, m (4200) seems to be depressed relative to its neighboring wavelengths near $\phi = 0.0$, and examination of figure 4 suggests that this is also true for the wavelengths at and adjacent to λ 5200. Since $\phi = 0.0$ is the phase of maximum line strength for both the REE and the Fe peak elements, these small variations in the λ 4200 and λ 5200 features may be entirely due to differential absorption. However, one would expect the variations to be much larger if they were due entirely to absorption by the aforementioned groups of elements, judging from the large changes that are seen in the shortward region of the Paschen continuum. Detailed spectrum synthesis calculations should be done to predict the expected changes precisely, once suitable model atmospheres become available.

As in previous papers of this series, we find evidence that there is flux redistribution from the far ultraviolet. For example, the Balmer jumps of all four of the Ap stars studied here correspond to higher temperatures than do the slopes of the Paschen continua when compared to

$\log g = 4.0$, solar composition model atmospheres. In addition, all four stars exhibit, to a greater or lesser degree, a general depression of all wavelengths shortward of about 5000 Å. It is not clear whether this depression also includes the λ 5200 feature. Figure 8 illustrates that this depression is not present in all stars whose red Paschen continua are the same. If the general depression in the blue-violet region is assumed to be due to differential absorption, it appears that the broad absorption features are not entirely due to the same effect. For example, in figure 8*a*, all three stars have very similar values of Δa, $\Delta a'$ and $\Delta\imath^*$, and the line blanketing coefficients of Wolff (1967) are similar for HD 111133 and 78 Vir; however, HD 111133 shows no general depression, while both 78 Vir and κ Psc do. In measuring the amount of line blanketing in heavily blanketed spectral regions, one does not necessarily observe the true continuum. The apparent high points may be lower than the continuum level. Thus, the measurements are most likely made relative to a pseudo-continuum. However, for the stars we are considering, the errors in determining the line blanketing in the blue-violet region should be similar, with the possible exception of HD 51418, which is heavily line blanketed. In comparing HD 50169 and HD 2453 with HD 51418 and 53 Cam, respectively (Figs. 8*b* and *c*) we find similar results; the first two stars show slightly stronger broad absorption features than do the second two stars while the first two stars show relatively less general absorption in the blue-violet. On the other hand, HD 204411 (Fig. 8*c*) matches 53 Cam in the red Paschen continuum but has much weaker broad absorption features as well as little general absorption in the blue-violet. The average energy distribution of HD 51418 approximately matches that of HD 110066 but at REE minimum, its blue-violet region is closer to that of HD 2453, while at REE maximum it displays a greater depression in this region than do any of the other stars (Fig. 8*b*). There is no corresponding change in the strength of the λ 5200 feature over the cycle of variation of HD 51418. The general conclusion that can be made from these comparisons is that neither the temperature (as derived from the slope of the red end of the Paschen continuum) nor the inferred amount of line blanketing in the blue-violet is strongly correlated with the strength of the broad absorption features in the Ap stars we have studied so far. Further discussion of this subject will be carried out in a later paper of this series.

The star HD 51418 is by far the most peculiar of the stars studied in papers I-XII. It shows the largest variation in the optical energy distribution with phase, has the largest amplitude photometric variations and exhibits a spectrum wherein the heavy REE are enhanced relative to the lighter REE. In this last characteristic it is matched only by HR 465 and α^2 CVn. These stars additionally show strong spectrum variations of the REE. However, the long period of HR 465 and the 20″ separation of α^1 and α^2 CVn make both of these stars difficult to study photometrically. It is worthwhile to further investigate these two stars as well as HD 51418, however, since all three should provide some important clues to the relationship between the spectrum peculiarities of Ap stars and the nature of the broad absorption features.

Acknowledgements. — The authors wish to thank the directors of Kitt Peak National Observatory and Mt. Wilson Observatory of the Carnegie Institution of Washington for the observing time needed for this series of papers. We are also grateful to Dr. H. M. Maitzen, our referee, who made a number of helpful comments and transmitted to us some of his photometric data prior to publication. Aspects of this project have been supported by the Citadel Development Foundation and the University of Nevada, Las Vegas. Since July 1981 this work was partially supported by NSF Grant AST 8106030 (S. J. A. principal investigator).

Appendix. — REVISION OF SYNTHETIC COLOR CALCULATIONS AND CRITERIA OF PRESENCE FOR THE λ 4200 AND λ 5200 BROAD CONTINUUM ABSORPTION FEATURES. — Paper I, paper III and paper IV have introduced photometric indices that can be used to detect the λ 4200 and λ 5200 broad continuum features of the Ap stars. The preliminary criteria of presence use the *b-y* colors which are synthesized from the spectrophotometry (see, e.g., Adelman, 1978). Recently, Adelman and Pyper (1983) have reexamined the relation between the synthesized and observed *b-y* colors in order to better derive the colors from spectrophotometry.

As we have a slightly larger number of normal star scans than when the criteria of presence for the various indices were established, and as we have made slight adjustments to the *b-y* values, we now reexamine the criteria of presence. We use the same sets of stars as were used for the examination of the *u-b* and *b-y* colors by Adelman and Pyper (1983), specifically, the 13 stars in Adelman, Pyper and White (1980) observed by D. M. P. (hereafter, Grid 1); and the 53 normal stars with at least 20 wavelength points in the region 4032-7100 Å (hereafter, Grid 2). Maitzen's Δa index (1976) is a measure of the strength of the λ 5200 broad continuum feature. It compares the flux near the center of the wavelength region affected with that in two wings. The other spectrophotometric indices, $\Delta a'$ to measure the λ 5200 feature and $\Delta\imath$, $\Delta\imath^*$, and $\Delta\imath^{**}$ to measure the λ 4200 feature, are defined in papers I, III and IV. Table AI summarizes the new relationships for normal stars, in general of the form $x_0 = a + b(b-y) + c(b-y)^2$. The criteria of presence are for $\Delta x = x - x_0$, where « x » represents the index measured for the Ap star. Further comments on the individual indices are as follows :

1) Δa : When allowance is made for the corrections in synthesizing *b-y*, the difference between the new relation for a_0 (Grid 2) and the one given in paper I for the normal stars is at most $0^m.001$, which occurs in the F stars. Forty-nine of the fifty-three stars have a values within $0^m.008$ of the mean relation. Of the four stars with larger differences, two have negative Δa ($= a - a_0$) values and two have positive ones. Perhaps these latter two stars (23 UMa and δ UMa) are slightly metal rich. The criteria of presence (Table AI) were based on the largest Δa value for a normal star, which is $0^m.012$. The Δa values calculated using the relation for Grid 1 compared to those from the Grid 2 relation differ by $0^m.002$ at most and $0^m.001$ on the average. The largest Δa value found for the Grid 1 stars is $0^m.003$, thus they are consistent with the criteria of presence given in table AI.

2) $\Delta a'$: In the a'_0 relationship for Grid 2, the largest deviation from the mean line is exhibited by ρ Gem ($-0^m.020$). If it is excluded from the sample, the rms scatter is reduced to $0^m.006$. Only two stars, HR 1427 and δ UMa, show positive deviations greater than $0^m.009$. Their values are $0^m.012$, on which the criteria for presence in table AI are based. When allowance is made for the b-y synthesis correction, the old and new $\Delta a'$ values differ by no more than $0^m.004$. This occurs in the intermediate F stars where the new values are $0^m.004$ smaller. The difference decreases towards the earlier stars, but in the early B stars the new values are $0^m.001$ larger. The $\Delta a'$ values calculated with the Grid 1 relation as compared to the Grid 2 relation differ by $0^m.008$ at most and $0^m.002$ on the average. The largest $\Delta a'$ values found for the Grid 1 sample is $0^m.007$ (Grid 1 relation) and $0^m.013$ (Grid 2 relation), which is in agreement with the criteria adopted in table AI.

3) $\Delta\iota$: (Both this and the discussion on $\Delta\iota^*$ refer only to the Grid 2 sample.) Four stars have $|\Delta\iota| > 0^m.013$, only one of which, η Lep, has a positive deviation ($0^m.016$), on which the criteria of presence are based. The new $\Delta\iota$ values are $0^m.003$ greater than the old values at $b\text{-}y = -0^m.10$. The differences decrease and then become negative with increasing b-y values. At $b\text{-}y = 0^m.10$, the new values are $0^m.001$ larger than the old ones while at $b\text{-}y = 0^m.15$, they are $0^m.004$ larger and at $b\text{-}y = 0^m.25$, they are $0^m.016$ larger. The new criterion of presence indicates that some λ 4200 features which were previously considered marginal are now considered to be present. This is in accord with the spectrophotometric results.

4) $\Delta\iota^*$: The largest deviation from the mean relation is for 23 UMa, where $\Delta\iota^* = -0.029$. If it is eliminated, then the rms scatter is $0^m.008$. Seven stars deviate more than $0^m.011$ of which only two stars, 21 Peg ($0^m.014$) and 21 Lyn ($0^m.020$) have positive deviations, on which the criteria of presence are based. The new $\Delta\iota^*$ values are within $0^m.001$ of the old values for $-0^m.05 < (b\text{-}y) < 0^m.15$. In the intermediate F stars ($b\text{-}y = 0^m.25$), the new values are $0^m.007$ smaller, while in the early B stars ($b\text{-}y = -0^m.10$), they are $0^m.005$ smaller.

5) $\Delta\iota^{**}$: The $\Delta\iota^{**}$ index is less sensitive than the other two indices in detecting weak λ 4200 features, as it does not use the λ 4200 point. For the Grid 2 sample, seven stars show deviations greater than $0^m.014$ from the mean relation. The largest of these is for 23 UMa, a deviation of $-0^m.034$. The two greatest positive deviations are $0^m.020$ for 21 Lyn and $0^m.017$ for 45 Boo, on which the criteria of presence are based. The new and old $\Delta\iota^{**}$ relations differ by $0^m.001$ or less for $0^m.00 < b\text{-}y < 0^m.10$. For $0^m.10 < b\text{-}y < 0^m.20$, the new relation gives values that are larger by $0^m.006$, while at $b\text{-}y = 0^m.25$, they are $0^m.010$ larger.

For the Grid 1 sample, θ And has the largest $\Delta\iota^{**}$ value, $0^m.011$. For $b\text{-}y = 0^m.03$, the $\Delta\iota^{**}$ values obtained by use of this relation and that for Grid 2 are within $0^m.003$. However, for $b\text{-}y = 0^m.04$, the Grid 2 relation gives considerably more negative $\Delta\iota^{**}$ values. For example, the difference is $0^m.011$ for τ Vir ($b\text{-}y = 0^m.066$) and $0^m.027$ for α Cep ($b\text{-}y = 0^m.122$). Since there are more stars in the Grid 2 sample, we adopt the criteria of presence for that sample in the case of $\Delta\iota^{**}$. Caution should be used in applying the $\Delta\iota^{**}$ criteria to stars with $b\text{-}y > 0^m.05$ that have been observed using Grid 1.

References

Abt, H. A., Chaffee, F. H., Suffolk, K. G. : 1972, *Astrophys. J.* **175,** 779.
Adelman, S. J. : 1978, *Astrophys. J.* **222,** 547.
Adelman, S. J. : 1979, *Astron. J.* **84,** 857 (Paper I).
Adelman, S. J. : 1981a, *Astron. Astrophys. Suppl. Ser.* **43,** 183 (Paper IX).
Adelman, S. J. : 1981b, *Astron. Astrophys. Suppl. Ser.* **44,** 265 (Paper X).
Adelman, S. J. : 1981c, *Astron. Astrophys. Suppl. Ser.* **44,** 309 (Paper XI).
Adelman, S. J., Pyper, D. M. : 1979, *Astron. J.* **84,** 1726 (Paper III).
Adelman, S. J., Pyper, D. M. : 1983, in preparation.
Adelman, S. J., Pyper, D. M., White, R. E. : 1980, *Astrophys. J. Suppl. Ser.* **43,** 491.
Babcock, H. W. : 1947, *Astrophys. J.* **105,** 105.
Babcock, H. W. : 1958, *Astrophys. J. Suppl. Ser.* **3,** 141.
Borra, E. F., Landstreet, J. D. : 1977, *Astrophys. J.* **212,** 141.
Borra, E. F., Landstreet, J. D. : 1980, *Astrophys. J. Suppl. Ser.* **42,** 421.
Cameron, R. C. : 1966, *Georgetown Obs. Monogr.* **21.**
Crawford, D. L., Barnes, J. V. : 1970, *Astron. J.* **75,** 978.
Crawford, D. L., Mander, J. : 1966, *Astron. J.* **71,** 114.
Deutsch, A. J. : 1947, *Astrophys. J.* **105,** 283.
Faraggiana, R. : 1973, *Astron. Astrophys.* **22,** 265.
Gulliver, A. F. : 1972, *Bull. Am. Astron. Soc.* **4,** 25.
Gulliver, A. F., Winzer, J. E. : 1973, *Astrophys. J.* **183,** 701.
Hardorp, J. : 1976, in *Physics of Ap Stars,* IAU Coll. 32, Vienna, ed., W. W. Weiss, H. Jenkner and H. J. Wood, p. 627.
Hensberge, H., van Rensbergen, W., Goossens, M., Deridder, G. : 1979, *Astron. Astrophys.* **75,** 83.
Hensberge, H., Maitzen, H. M., Deridder, G., Gerbaldi, M., Delmas, F., Renson, P., Doom, C., Weiss, W. W., Morguleff, N. : 1981, *Astron. Astrophys. Suppl. Ser.* **46,** 151.
Huchra, J. P. : 1972, *Astrophys. J.* **174,** 435.
Jones, T. J., Wolff, S. C., Bonsack, W. K. : 1974, *Astrophys. J.* **190,** 579.
Jugaku, J., Sargent, W. L. W. : 1968, *Astrophys. J.* **151,** 259.

KURUCZ, R. L. : 1979, *Astrophys. J. Suppl. Ser.* **40,** 1.
MAITZEN, H. M. : 1976, *Astron. Astrophys.* **51,** 223.
MAITZEN, H. M., WEISS, W. W., JENKNER, H., KLUKE, J. : 1978, *Astron. Astrophys.* **69,** 103.
MIHALAS, D., HENSHAW, J. L. : 1966, *Astrophys. J.* **144,** 25.
MORGAN, W. W. : 1932, *Astrophys. J.* **76,** 275.
PETERSON, D. M. : 1970, *Astrophys. J.* **161,** 685.
PRESTON, G. W. : 1969a, *Astrophys. J.* **157,** 247.
PRESTON, G. W. : 1969b, *Astrophys. J.* **158,** 243.
PRESTON, G. W. : 1970, in *Stellar Rotation,* A. Slettebak, ed. (Dordrecht, Holland D. Reidel Pub. Co.), p. 254.
PRESTON, G. W., STEPIEN, K. : 1968, *Astrophys. J.* **151,** 583.
RAKOS, K. D. : 1962, *Lowell Obs. Bull.* **5,** 227.
RELYEA, L. J., KURUCZ, R. L. : 1978, *Astrophys. J. Suppl. Ser.* **37,** 45.
SCHOLZ, G. : 1978, *Publ. Astron. Inst. Czech. Acad. Sci.* No. 54, ed., J. Grygar and Z. Mikulasek, p. 10.
SEARLE, L., SARGENT, W. L. W. : 1964, *Astrophys. J.* **139,** 753.
STEPIEN, K. : 1968, *Astrophys. J.* **154,** 945.
STRÖMGREN, B., PERRY, C. L. : 1965, *Institute for Advanced Study* (Princeton, NJ) 2nd Version (unpublished).
VAN DIJK, W., KERSSIES, A., HAMMERSCHLAG-HENSBERGE, G., WESSELIUS, P. R. : 1978, *Astron. Astrophys.* **66,** 187.
VAN GENDEREN, A. M. : 1971, *Astron. Astrophys.* **14,** 48.
WHITE, R. E., PYPER, D. M., ADELMAN, S. J. : 1980, *Astron. J.* **85,** 836 (Paper IV).
WINZER, J. E. : 1974, thesis, Univ. of Toronto.
WOLFF, S. C. : 1967, *Astrophys. J. Suppl. Ser.* **15,** 21.
WOLFF, S. C., WOLFF, R. J. : 1971, *Astron. J.* **76,** 422.

TABLE I. — *Summary of Phase Variations : HD 51418, 53 Cam, 78 Vir and κ Psc.*

Star	i	Spectrum Variations	Photometric Amplitude (mag)	Magnetic Amplitude (kgauss)	References
HD 51418	45°	large, esp. REE	0.18 (y)	0.9	a;b;c,n;d
53 Cam	60°	large	0.065 (u)	10.0	e,f,g;h;i,n;j
78 Vir	22°	Ca II K moderate, others small	0.035 (u)	0.9	k;l;i;m
κ Psc	8°	small	0.02: (u)	0 or small	b;o;n,p;k

Note : References to Columns 2-5, respectively, are separated by « ; ». The references are :

a. Hardorp (1976)
b. Preston (1970)
c. Gulliver and Winzer (1973)
d. Jones *et al.* (1974)
e. Huchra (1972)
f. Borra and Landstreet (1977)
g. Hensberge *et al.* (1979)
h. Faraggiana (1973)
i. Wolff and Wolff (1971)
j. Preston and Stepien (1968)
k. Borra and Landstreet (1980)
l. Deutsch (1947)
m. Preston (1969b)
n. This paper, photometry
o. Babcock (1958)
p. Van Genderen (1971).

TABLE II. — *Journal of observations for spectrophotometry.*

Star	Scan Number	Heliocentric Julian Date	Phase	Observatory	Observer
HD 51418	1	2442143.646	0.871	Kitt Peak	DMP
	2	2442144.635	0.053	Kitt Peak	DMP
	3	2442146.659	0.426	Kitt Peak	DMP
	4	2443585.663	0.050	Kitt Peak	SJA
	5	2444569.021	0.884	Kitt Peak	SJA
	6	2444571.020	0.252	Kitt Peak	SJA
	7	2444572.027	0.437	Kitt Peak	SJA
	8	2444573.021	0.620	Kitt Peak	SJA
	9	2444574.974	0.979	Kitt Peak	SJA
	10	2444651.839	0.114	Kitt Peak	SJA/DMP
	11	2444653.867	0.487	Kitt Peak	SJA/DMP
	12	2444654.672	0.635	Kitt Peak	SJA/DMP
	13	2444654.826	0.664	Kitt Peak	SJA/DMP
	14	2444655.688	0.822	Kitt Peak	SJA/DMP
	15	2444655.829	0.848	Kitt Peak	SJA/DMP
53 Cam	1	2441323.851	0.251	Mt. Wilson	DMP
	2	2441401.679	0.947	Kitt Peak	DMP
	3	2441404.668	0.320	Kitt Peak	DMP
	4	2441415.668	0.690	Kitt Peak	DMP
	5	2441795.663	0.032	Kitt Peak	DMP
	6	2441796.731	0.165	Kitt Peak	DMP
	7	2442111.857	0.424	Kitt Peak	DMP
	8	2442143.670	0.388	Kitt Peak	DMP
	9	2442144.654	0.510	Kitt Peak	DMP
	10	2442145.720	0.643	Kitt Peak	DMP
	11	2443583.740	0.798	Kitt Peak	SJA
	12	2443584.721	0.920	Kitt Peak	SJA
	13	2443585.689	0.040	Kitt Peak	SJA
78 Vir	1	2441401.866	0.201	Kitt Peak	DMP
	2	2441404.868	0.008	Kitt Peak	DMP
	3	2441415.880	0.966	Kitt Peak	DMP
	4	2441416.850	0.227	Kitt Peak	DMP
	5	2441417.871	0.501	Kitt Peak	DMP
	6	2441488.750	0.544	Mt. Wilson	DMP
	7	2442120.913	0.389	Kitt Peak	SJA
	8	2442121.912	0.658	Kitt Peak	SJA
	9	2442409.066	0.808	Kitt Peak	SJA
	10	2442522.715	0.343	Kitt Peak	SJA
	11	2442526.695	0.141	Kitt Peak	SJA
	12	2442527.704	0.683	Kitt Peak	SJA
	13	2442528.700	0.951	Kitt Peak	SJA
	14	2442529.736	0.229	Kitt Peak	SJA
κ Psc	1	2441558.904	0.895	Mt. Wilson	DMP
	2	2441560.946	0.385	Mt. Wilson	DMP
	3	2441561.853	0.934	Mt. Wilson	DMP
	4	2441562.888	0.703	Mt. Wilson	DMP
	5	2441577.832	0.234	Mt. Wilson	DMP
	6	2441578.831	0.942	Mt. Wilson	DMP
	7	2441616.744	0.717	Kitt Peak	DMP
	8	2443061.774	0.587	Kitt Peak	SJA
	9	2443063.737	0.941	Kitt Peak	SJA
	10	2443066.689	0.985	Kitt Peak	SJA

Note : D.M.P. and S.J.A./D.M.P. used bandpasses of 20 Å in the 2nd order ; S.J.A. used 30 Å in the 2nd order. The 1st order bandpasses were twice as great.

TABLE III. — *Comparison of Strömgren uvby photometry for Ap and comparison stars.*

Star	HD	V	u-b	b-y	m_1	n	References
	51418	---	1.208	0.030	---	15	This paper: spectrophotometry
		6.671	1.211	0.037	0.217	17	This paper: photometry
	(σ)	(0.061)	(0.013)	(0.017)	(0.025)		
60 Aur	50037	6.311	1.469	0.321	0.175[1]	17	This paper: photometry
	(σ)	(0.020)	(0.008)	(0.006)	(0.011)		
		---	1.445	0.331	---	1	Cameron (1966)
53 Cam	65339	---	1.409	0.044	---	11	This paper: spectrophotometry
		6.024	1.411	0.054	0.267[2]	11	This paper: photometry
	(σ)	(0.013)	(0.017)	(0.004)	(0.013)		
		6.05	1.396	0.059	0.266	14	Wolff and Wolff (1971)
HR 3106	65301	5.779	1.379	0.266	0.168[3]	10	This paper: photometry
	(σ)	(0.015)	(0.008)	(0.004)	(0.008)		
		5.75	1.371	0.264	0.177	14	Wolff and Wolff (1971)
		---	1.363	0.264	0.168	2	Strömgren and Perry (1965)
78 Vir	118022	---	1.376	-0.026	---	14	This paper: spectrophotometry
		4.90	1.344	0.000	0.207	15	Wolff and Wolff (1971)
		---	1.373	-0.007	0.226	2	Strömgren and Perry (1965)
		---	1.376	-0.010	0.231	3	Cameron (1966)
κ Psc	220825	---	1.330	-0.012	---	10	This paper: spectrophotometry
		4.924	1.299	-0.002	0.218	16	This paper: photometry
	(σ)	(0.012)	(0.011)	(0.004)	(0.013)		
		---	1.299	-0.006	0.218	5	Strömgren and Perry (1965)
		---	1.324	0.005	0.212	2	Cameron (1966)
	221318	7.133	1.367	0.282	0.170	16	This paper: photometry
	(σ)	(0.016)	(0.013)	(0.007)	(0.009)		

Notes : The comparison star for 78 Vir was not included, since D.M.P. did no *uvby* photometry on it :
([1]) $n = 13$.
([2]) $n = 7$.
([3]) $n = 6$.

TABLE IV. — *Temperature estimates.*

Star	Spectrophotometric Fitting PC[1]	BJ[3]	u-b[4]	Literature	References[5]
HD 51418	9000 K	11500 K	10400 K	---	---
53 Cam	8500 K	10250 K	9400 K	8400 K	c
78 Vir	9500 K[2]	10000 K	9600 K	9700-10700 K	b,d,e
κ Psc	9500 K	10250 K	9800 K	9500-10500 K	a,b,d,e

Notes :
([1]) Red end of Paschen continuum matched to model (Kurucz, 1979).
([2]) $T = 9250$ K, $\log g = 4.5$ may fit this energy distribution globally.
([3]) Blue end of Paschen continuum (model) matched to λλ 4032-4255.
([4]) Synthesized *u-b* values compared to those of Relyea and Kurucz (1978).
([5]) References are : a = Searle and Sargent (1964) ; b = Mihalas and Henshaw (1966) ; c = Faraggiana (1973) ; d = Wolff (1967) ; e = Jugaku and Sargent (1968).

TABLE V. — *Four-color photometry of HD 51418, 53 Cam and κ Psc.*

Star	Heliocentric Julian Date	Phase	Δy[1]	$\Delta(b-y)$[1]	$\Delta(u-b)$[1]	m_1	β
HD 51418	2444217.946	0.324	0.397	-0.286	-0.259	0.179	2.786
	2444221.948	0.060	0.256	-0.257	-0.245	0.250:	2.757
	2444222.918	0.238	0.370	-0.278	-0.251	0.244:	2.776
	2444338.653	0.521	0.407	-0.301	-0.277	0.143:[2]	2.785:
	2444339.647	0.704	0.363	-0.291	-0.277	0.166:[2]	2.778
	2444340.646	0.888	0.259:	-0.271	-0.247	0.214:[2]	2.765
	2444342.651	0.256	0.366	-0.284	-0.261	0.207	2.795
	2444343.655	0.441	0.421	-0.313	-0.262	0.160:[2]	2.785
	2444588.956	0.550	0.416	-0.315	-0.272	0.185	2.790:
	2444589.926	0.729	0.354	-0.297	-0.268	0.222	2.773
	2444590.906	0.909	0.258	-0.263	-0.241	0.241	2.750
	2444928.990	0.081	0.267	-0.275	-0.238	0.251	2.756
	2444929.963	0.260	0.387	-0.291	-0.258	0.201	2.793
	2444931.977	0.630	0.386	-0.298	-0.271	0.187	2.796
	2444932.953	0.810	0.305	-0.276	-0.260	0.206	2.760
	2444933.956	0.994	0.245	-0.248	-0.244	0.228	2.743
	2444934.872	0.163	0.323	-0.292	-0.259	0.219	2.772
53 Cam	2444217.969	0.812	---	---	---	---	2.866
	2444222.941	0.432	---	---	---	---	2.825:
	2444338.676	0.851	0.235	-0.215	0.056	0.259:[2]	2.861
	2444339.665	0.974	0.239	-0.206	0.039	0.238:[2]	2.862
	2444340.662	0.098	0.246	-0.214	0.016	0.244:[2]	2.868:
	2444342.669	0.348	0.237	-0.215	0.007	0.243:[2]	2.842
	2444343.670	0.473	---	---	---	---	2.835
	2444588.970	0.033	0.231:	-0.208:	0.033	0.281:	2.870
	2444589.950	0.156	---	---	---	---	2.858
	2444590.918	0.276	---	---	---	---	2.836
	2444929.002	0.396	5.977:[3]	0.058:[3]	1.383:[3]	0.263:	2.841:
	2444929.978	0.518	0.232	-0.209	0.035	0.274	2.856
	2444931.986	0.768	0.220	-0.201	0.052	0.276	2.866
	2444932.975	0.891	0.240	-0.207	0.041	0.268	2.855
	2444933.970	0.015	0.248	-0.221	0.038	0.269	2.843
	2444934.880	0.128	0.236:	-0.221:	0.027:	0.241:	2.863:
κ Psc	2444217.578	0.308	-2.247	-0.277	-0.079	0.239	2.887
	2444221.584	0.153	-2.258	-0.280	-0.068:	0.251:	2.863
	2444222.588	0.868	-2.233	-0.281	-0.066	0.222:	2.867
	2444588.669	0.327	-2.266	-0.284	-0.077	0.218	2.879
	2444589.582	0.887	-2.243	-0.280	-0.084	0.220	2.876
	2444590.567	0.569	-2.237	-0.282	-0.060:	0.201	2.872
	2444927.670	0.519	-2.249	-0.310	-0.054	0.225	2.875
	2444927.719	0.602	-2.248	-0.286	-0.067	0.208	2.867
	2444929.610	0.833	-2.256	-0.281	-0.076	0.217	2.868
	2444929.682	0.956	-2.247:	-0.287	-0.075	0.216	2.875
	2444931.729	0.453	-2.255	-0.284	-0.057	0.214	2.878
	2444932.591	0.926	-2.257	-0.283	-0.071	0.211	2.865
	2444932.651	0.029	-2.257	-0.276	-0.079	0.207	2.862
	2444933.604	0.657	-2.249	-0.276	-0.067	0.218	2.867
	2444933.683	0.792	-2.246	-0.291	-0.056	0.215	2.866:
	2444934.603	0.364	-2.251	-0.295	-0.058	0.204	2.869

Notes :

([1]) « Δ » = star — comparison.
([2]) Calculated from $\overline{m}_1$ (comparison) + Δm_1, all others are for star.
([3]) No comparison observed ; *y*, *b-y* and *u-b* values are for star.

TABLE VI. — *Continuous energy distributions (− 2.5 log F_ν/F_{5000}) for HD 51418.*

λ(A)	1	2	3
3390	1.088	1.093	1.054
3448	1.066	1.053	1.026
3509	1.034	1.041	1.006
3571	0.991	0.996	0.979
3636	0.950	0.941	0.951
4032	0.020	0.057	-0.123
4167	-0.004	0.020	-0.090
4255	0.025	0.038	-0.077
4464	-0.045	-0.050	-0.104
4566	-0.041	-0.044	-0.076
4785	-0.055	-0.060	-0.064
5000	0.000	0.000	0.000
5264	0.088	0.076	0.067
5556	0.052	0.039	0.074
5840	0.093	0.076	0.090
6058	0.135	0.113	0.154
6370	0.198	0.193	0.209
6800	0.251	0.233	0.261
7100	0.291	0.282	0.302
7530	0.375	0.353	0.389
7850	0.412	0.373	0.400
u-b	1.216	1.225	1.219
b-y	0.041	0.050	0.013
Δa	0.030	0.026	0.015
Δa'	0.055	0.052	0.046
Δ_1**	0.008	0.007	0.023

TABLE VI *(continued)*.

λ(Å)	4	5	6	7	8	9	10	11	12	13	14	15	Average
3300	1.087	1.076	1.060	1.040	1.024	1.094	1.074	1.025	1.039	1.039	1.060	1.089	1.059
3390	1.091	1.077	1.055	1.040	1.032	1.098	1.060	1.023	1.041	1.045	1.060	1.090	1.063
3448	1.059	1.046	1.032	1.015	1.005	1.065	1.061	0.999	1.029	1.006	1.043	1.058	1.038
3509	1.019	1.010	0.985	0.991	0.954	1.028	1.001	0.964	0.981	0.965	0.991	1.020	0.999
3540	---	0.963	0.963	0.973	0.947	0.973	0.983	0.961	0.958	0.951	0.974	0.972	0.965
3571	0.989	0.976	0.987	0.993	0.961	0.997	0.986	0.967	0.973	0.964	0.981	0.982	0.975
3636	0.938	0.930	0.939	0.959	0.927	0.950	0.945	0.927	0.944	0.943	0.942	0.940	0.942
3704	0.901	0.885	0.910	0.895	0.879	0.889	0.911	0.905	0.905	0.900	0.902	0.905	0.899
4032	0.065	0.026	-0.045	-0.114	-0.088	0.074	0.027	-0.138	-0.096	-0.088	-0.014	0.009	-0.029
4167	0.054	0.007	-0.050	-0.067	-0.068	0.050	-0.010	-0.098	-0.067	-0.059	-0.018	-0.014	-0.028
4200	0.074	0.025	-0.023	-0.061	-0.046	0.071	0.036	-0.079	-0.042	-0.036	0.027	0.029	-0.002
4255	0.031	0.005	-0.040	-0.065	-0.070	0.033	0.001	-0.071	-0.053	-0.053	-0.014	-0.008	-0.021
4340	---	0.293	0.323	0.337	0.317	0.314	0.438	0.476	0.482	0.470	0.439	0.432	---
4464	-0.063	-0.073	-0.094	-0.108	-0.100	-0.050	-0.084	-0.122	-0.093	-0.091	-0.069	-0.058	-0.080
4566	-0.036	-0.054	-0.069	-0.084	-0.079	-0.053	-0.070	-0.099	-0.058	-0.072	-0.049	-0.079	-0.064
4673	-0.061	-0.066	-0.078	-0.075	-0.069	-0.062	-0.075	-0.100	-0.069	-0.063	-0.069	-0.074	-0.072
4785	-0.043	-0.064	-0.064	-0.062	-0.066	-0.061	-0.089	-0.070	-0.056	-0.061	-0.071	-0.081	-0.064
4861	---	0.295	0.348	0.376	0.370	0.289	0.455	0.513	0.484	0.461	0.449	0.419	---
4935	-0.043	-0.055	-0.039	-0.047	-0.040	-0.037	-0.058	-0.054	-0.036	-0.044	-0.054	-0.058	-0.047
4975	---	-0.041	-0.035	-0.033	-0.024	-0.039	-0.052	-0.039	-0.030	-0.030	-0.032	-0.050	-0.037
5000	0.000	0.000	0.000	0.000	0.000	0.000	0.000	0.000	0.000	0.000	0.000	0.000	0.000
5060	---	-0.005	0.013	0.009	0.001	-0.003	-0.003	-0.001	0.014	0.013	-0.004	-0.019	0.001
5128	0.053	0.054	0.039	0.050	0.054	0.043	0.046	0.036	0.036	0.049	0.055	0.047	0.047
5200	0.102	0.091	0.086	0.073	0.082	0.093	0.081	0.082	0.091	0.101	0.086	0.099	0.088
5232	---	0.058	0.075	0.066	0.084	0.069	0.057	0.058	0.095	0.092	0.081	0.070	0.073
5264	0.069	0.057	0.065	0.064	0.064	0.064	0.057	0.040	0.079	0.074	0.075	0.057	0.066
5360	0.054	0.047	0.070	0.078	0.065	0.056	0.034	0.048	0.062	0.074	0.057	0.044	0.057
5470	0.054	0.040	0.060	0.073	0.062	0.042	0.041	0.062	0.070	0.066	0.050	0.052	0.056
5556	0.052	0.045	0.075	0.085	0.078	0.035	0.031	0.058	0.075	0.085	0.054	0.034	0.058
5700	0.062	0.039	0.073	0.079	0.097	0.035	0.049	0.077	0.082	0.103	0.054	0.040	0.066
5800	---	0.081	0.129	0.120	0.132	0.096	0.100	0.135	0.127	0.142	0.099	0.105	0.115
5840	0.078	0.054	0.097	0.097	0.106	0.065	0.070	0.103	0.112	0.111	0.073	0.070	0.086
5875	---	0.086	0.120	0.135	0.133	0.087	0.086	0.114	0.125	0.151	0.096	0.097	0.112
6020	0.115	0.093	0.122	0.148	0.148	0.120	0.112	0.130	0.129	0.135	0.118	0.107	0.123
6058	---	0.109	0.136	0.146	0.154	0.117	0.112	0.154	0.155	0.168	0.129	0.111	0.135
6220	0.149	0.140	0.169	0.191	0.173	0.132	0.137	0.173	0.176	0.183	0.140	0.136	0.158
6300	0.165	0.159	0.173	0.195	0.197	0.145	0.168	0.182	0.187	0.203	0.167	0.155	0.175
6370	0.190	0.181	0.207	0.218	0.196	0.165	0.177	0.213	0.201	0.217	0.188	0.185	0.196
6440	---	0.201	0.218	0.244	0.235	0.196	0.210	0.235	0.228	0.237	0.223	0.199	0.221
6563	---	0.372	0.410	0.433	0.406	0.383	0.462	0.489	0.492	0.492	0.454	0.445	---
6650	0.212	0.213	0.246	0.244	0.241	0.204	0.202	0.239	0.240	0.245	0.213	0.201	0.225
6710	---	0.209	0.231	0.251	0.246	0.210	0.214	0.244	0.254	0.256	0.222	0.211	0.232
6800	0.255	0.219	0.245	0.267	0.261	0.230	0.209	0.248	0.267	0.282	0.231	0.228	0.246
7100	0.292	0.273	0.299	0.311	0.309	0.274	0.264	0.304	0.293	0.301	0.281	0.254	0.289
7530	---	---	---	---	---	---	0.364	0.388	0.374	0.388	0.359	0.353	0.371
7850	---	---	---	---	---	---	0.405	0.427	0.410	0.434	0.390	0.389	0.404
u-b	1.211	1.209	1.211	1.207	1.183	1.222	1.227	1.207	1.192	1.187	1.205	1.226	1.208
b-y	0.049	0.049	0.016	0.005	0.016	0.052	0.040	0.007	0.021	0.015	0.036	0.034	0.030
Δa	0.040	0.040	0.033	0.026	0.034	0.042	0.040	0.028	0.038	0.040	0.044	0.047	0.038
Δa'	0.034	0.045	0.038	0.037	0.034	0.045	0.052	0.014	0.040	0.039	0.060	0.049	0.042
Δι	0.008	-0.007	-0.002	0.018	0.014	-0.001	-0.009	0.008	0.012	0.015	0.011	-0.001	0.002
Δι*	0.055	0.031	0.032	0.050	0.037	0.040	0.035	0.044	0.038	0.042	0.041	0.027	0.036
Δι**	0.013	0.005	0.008	0.037	0.013	0.002	-0.001	0.037	0.024	0.022	0.006	-0.007	0.012

Note : Balmer line bandpasses were not used in the calculation of *u-b*, *b-y* and Δa.

TABLE VII. — *Continuous energy distributions ($-2.5 \log F_\lambda/F_{5000}$) for 53 Cam.*

λ(Å)	1	2	3	4	5	6	7	8	9	10
3390	---	1.231	1.235	1.274	1.269	1.291	1.277	1.265	1.295	1.316
3448	---	1.236	1.239	1.242	1.241	1.248	1.243	1.249	1.242	1.254
3509	---	1.177	1.141	1.183	1.184	1.179	1.184	1.174	1.189	1.211
3571	---	1.191	1.188	1.182	1.172	1.175	1.175	1.180	1.187	1.198
3636	---	1.153	1.130	1.142	1.146	1.145	1.128	1.141	1.146	1.148
4032	-0.064	-0.073	-0.072	-0.073	-0.075	-0.072	-0.083	-0.065	-0.066	-0.042
4167	-0.034	0.006	-0.020	0.003	-0.028	-0.002	-0.012	0.001	-0.002	0.005
4255	0.009	0.006	-0.005	0.016	-0.011	0.006	0.014	0.012	0.016	0.007
4464	-0.063	-0.081	-0.063	-0.028	-0.044	-0.040	-0.033	-0.041	-0.041	-0.046
4566	-0.077	-0.068	-0.098	-0.040	-0.057	-0.063	-0.060	-0.053	-0.049	-0.030
4785	-0.086	-0.110	-0.107	-0.102	-0.098	-0.084	-0.107	-0.096	-0.093	-0.106
5000	0.000	0.000	0.000	0.000	0.000	0.000	0.000	0.000	0.000	0.000
5264	0.069	0.106	0.119	0.103	0.076	0.095	0.061	0.101	0.096	0.092
5556	0.042	0.033	0.051	0.034	0.041	0.053	0.039	0.068	0.048	---
5840	0.038	0.029	0.041	0.037	0.038	0.055	0.045	0.059	0.057	0.049
6058	0.080	0.063	0.066	0.067	0.058	0.089	0.072	0.081	0.077	0.079
6370	0.120	0.116	0.144	0.139	0.145	0.161	0.126	0.149	0.145	0.139
6800	0.144	0.157	0.164	0.175	0.178	0.192	0.167	0.180	0.164	0.157
7100	0.158	0.192	0.201	0.203	0.204	0.220	0.201	0.212	0.206	0.208
7530	0.232	0.250	0.266	0.267	0.293	0.281	0.332	0.278	0.273	0.291
7850	0.251	0.284	0.309	0.312	0.294	0.302	0.343	0.343	0.304	0.308
u-b	---	1.411	1.415	1.418	1.423	1.433	1.429	1.413	1.437	1.451
b-y	0.024	0.006	-0.023	0.027	0.027	0.015	0.029	0.003	0.021	0.018
Δa	0.025	0.050	0.054	0.047	0.030	0.036	0.023	0.038	0.039	0.034
Δa'	0.082	0.140	0.151	0.125	0.095	0.101	0.081	0.114	0.105	0.112
$\Delta\imath$**	0.042	0.073	0.049	0.056	0.034	0.053	0.056	0.040	0.042	0.028

λ(Å)	11	12	13	Average
3300	1.258	1.234	1.239	1.244
3390	1.287	1.268	1.256	1.272
3448	1.238	1.247	1.234	1.243
3509	1.201	1.188	1.169	1.182
3571	1.175	1.198	1.196	1.185
3636	1.158	1.146	1.141	1.144
3704	1.115	1.063	1.056	1.078
4032	-0.073	-0.057	-0.064	-0.068
4167	0.012	0.007	0.004	-0.005
4200	0.039	0.038	0.041	0.039
4255	0.009	-0.010	-0.017	0.004
4464	-0.049	-0.072	-0.085	-0.053
4566	-0.055	-0.066	-0.061	-0.060
4673	-0.061	-0.077	-0.063	-0.067
4785	-0.114	-0.097	-0.095	-0.100
4935	-0.045	-0.045	-0.038	-0.043
5000	0.000	0.000	0.000	0.000
5128	-0.024	-0.007	0.017	-0.005
5200	0.072	0.061	0.064	0.066
5264	0.073	0.071	0.073	0.087
5360	0.044	0.039	0.042	0.042
5470	0.018	0.023	0.033	0.025
5556	0.030	0.037	0.054	0.044
5700	0.023	0.017	0.027	0.022
5840	0.031	0.026	0.040	0.042
6020	0.064	0.052	0.062	0.059
6058	---	---	---	0.074
6220	0.090	0.095	0.112	0.099
6300	0.099	0.100	0.109	0.103
6370	0.126	0.124	0.138	0.136
6650	0.147	0.140	0.159	0.149
6800	0.157	0.146	0.170	0.165
7100	0.194	0.187	0.199	0.199
7530	---	---	---	0.276
7850	---	---	---	0.305
u-b	1.408	1.416	1.400	1.409
b-y	0.062	0.043	0.042	0.044
Δa	0.043	0.035	0.032	0.042
Δa'	0.097	0.090	0.085	0.101
$\Delta\imath$	0.050	0.048	0.055	0.041
$\Delta\imath$*	0.075	0.080	0.090	0.070
$\Delta\imath$**	0.060	0.048	0.053	0.049

TABLE VIII. — *Continuous energy distributions (− 2.5 log F_λ/F_{5000}) for 78 Vir.*

λ(Å)	1	2	3	4	5	6	7	8
3300	---	---	---	---	---	---	1.201	1.195
3390	1.179	1.179	1.204	1.183	1.158	---	1.184	1.190
3448	1.190	1.184	1.173	1.179	1.175	---	1.184	1.181
3509	1.129	1.115	1.131	1.129	1.088	---	1.115	1.124
3571	1.148	1.135	1.128	1.141	1.126	---	1.129	1.131
3636	1.118	1.087	1.081	1.095	1.079	---	1.061	1.073
3704	---	---	---	---	---	---	1.023	1.022
4032	-0.156	-0.172	-0.172	-0.141	-0.141	-0.152	-0.147	-0.158
4167	-0.094	-0.113	-0.109	-0.121	-0.139	-0.128	-0.121	-0.103
4255	-0.089	-0.102	-0.090	-0.103	-0.096	-0.119	-0.111	-0.103
4464	-0.120	-0.117	-0.104	-0.124	-0.128	-0.146	-0.129	-0.129
4566	-0.098	-0.101	-0.088	-0.093	-0.100	-0.133	-0.125	-0.115
4785	-0.095	-0.089	-0.095	-0.090	-0.099	-0.103	-0.101	-0.093
5000	0.000	0.000	0.000	0.000	0.000	0.000	0.000	0.000
5264	0.114	0.108	0.105	0.092	0.104	0.084	0.076	0.088
5556	0.100	0.102	0.099	0.084	0.094	0.071	0.076	0.078
5840	0.122	0.108	0.112	0.126	0.102	0.087	0.102	0.100
6058	0.165	0.166	0.153	0.182	0.158	0.140	0.138	0.146
6370	0.228	0.230	0.227	0.242	0.211	0.198	0.204	0.193
6800	0.293	0.285	0.294	0.292	0.258	0.256	0.267	0.265
7100	0.347	0.334	0.321	0.333	0.314	0.310	0.320	0.307
7530	0.416	0.420	0.429	0.416	0.407	0.408	---	---
7850	0.467	0.467	0.469	---	0.435	0.432	---	---
u−b	1.374	1.364	1.380	1.369	1.348	---	1.390	1.381
b−y	-0.049	-0.046	-0.038	-0.025	-0.044	-0.041	-0.035	-0.032
Δa	0.039	0.035	0.034	0.030	0.036	0.032	0.023	0.028
Δa'	0.107	0.104	0.100	0.072	0.106	0.096	0.073	0.081
Δ_1**	0.048	0.040	0.042	0.016	0.015	0.018	0.019	0.019

λ(Å)	9	10	11	12	13	14	Average
3300	1.154	1.231	1.202	1.176	1.194	1.193	1.193
3390	1.180	1.218	1.192	1.188	1.190	1.183	1.187
3448	1.160	1.207	1.189	1.186	1.175	1.165	1.181
3509	1.095	1.153	1.122	1.103	1.116	1.104	1.117
3571	1.103	1.132	1.119	1.143	1.122	1.124	1.129
3636	1.049	1.094	1.082	1.080	1.079	1.079	1.081
3704	1.027	1.068	1.045	1.034	1.037	1.028	1.036
4032	-0.157	-0.154	-0.154	-0.138	-0.155	-0.143	-0.153
4167	-0.107	-0.129	-0.105	-0.104	-0.117	-0.109	-0.114
4200	-0.110	-0.097	-0.094	-0.082	-0.111	-0.099	-0.099
4255	-0.109	-0.108	-0.106	-0.099	-0.119	-0.103	-0.104
4464	-0.127	-0.148	-0.125	-0.111	-0.125	-0.130	-0.126
4566	-0.111	-0.091	-0.098	-0.084	-0.096	-0.086	-0.101
4785	-0.108	-0.081	-0.094	-0.086	-0.096	-0.078	-0.093
5000	0.000	0.000	0.000	0.000	0.000	0.000	0.000
5128	0.033	0.021	0.038	0.056	0.026	0.042	0.036
5264	0.081	0.092	0.092	0.096	0.086	0.100	0.094
5360	0.080	0.084	0.080	0.086	0.076	0.086	0.082
5470	0.082	0.089	0.063	0.078	0.075	0.084	0.078
5556	0.105	0.085	0.082	0.100	0.092	0.107	0.091
5840	0.106	0.093	0.096	0.112	0.104	0.126	0.107
6020	0.142	0.154	0.129	0.153	0.146	0.173	0.150
6058	---	---	---	---	---	---	0.156
6220	0.205	0.192	0.183	0.191	0.191	0.207	0.195
6370	0.210	0.213	0.199	0.208	0.195	0.229	0.214
6650	0.257	0.235	0.231	0.256	0.237	0.278	0.244
6800	0.296	0.243	0.254	0.271	0.249	0.298	0.273
7100	0.321	0.309	0.307	0.330	0.296	0.333	0.320
7530	---	---	---	---	---	---	0.415
7850	---	---	---	---	---	---	0.454
u−b	1.363	1.394	1.379	1.360	1.373	1.355	1.376
b−y	-0.040	-0.019	-0.017	-0.018	-0.021	-0.021	-0.026
Δa	0.022	0.024	0.032	0.032	0.024	0.029	0.029
Δa'	0.081	0.080	0.086	0.078	0.078	0.072	0.083
Δ_1	0.018	0.011	0.024	0.018	0.016	0.012	0.015
Δ_1*	0.050	0.047	0.049	0.040	0.036	0.042	0.044
Δ_1**	0.035	0.027	0.031	0.020	0.020	0.027	0.028

TABLE IX. — *Continuous energy distributions (− 2.5 log F_λ/F_{5000}) for κ Psc.*

λ(Å)	1	2	3	4	5	6	7
3390	---	---	---	---	---	---	1.191
3448	---	---	---	---	---	---	1.156
3509	---	---	---	---	---	---	1.116
3571	---	---	1.048	1.052	1.077	1.090	1.100
3636	---	---	1.023	1.018	1.038	1.039	1.061
4032	-0.136	-0.151	-0.134	-0.135	-0.143	-0.155	-0.119
4167	-0.097	-0.099	-0.101	-0.110	-0.112	-0.121	-0.091
4255	-0.099	-0.144	-0.101	-0.111	-0.095	-0.104	-0.081
4464	-0.140	-0.142	-0.122	-0.135	-0.103	-0.118	-0.099
4566	-0.094	-0.097	-0.094	-0.100	-0.067	-0.073	-0.055
4785	-0.071	-0.073	-0.072	-0.091	-0.065	-0.077	-0.066
5000	0.000	0.000	0.000	0.000	0.000	0.000	0.000
5264	0.066	0.077	0.084	0.078	0.090	0.090	0.094
5556	0.089	0.097	0.107	0.089	0.102	0.109	0.099
5840	0.123	0.129	0.127	0.118	0.133	0.130	0.135
6058	0.164	0.177	0.172	0.157	0.176	0.173	0.176
6370	0.225	0.236	0.223	0.215	0.231	0.235	0.218
6800	0.276	0.289	0.298	0.290	0.289	0.299	0.291
7100	0.328	0.337	0.346	0.336	0.339	0.356	0.339
7530	0.406	0.418	0.428	0.409	0.450	0.444	0.421
7850	---	0.452	0.470	0.459	0.458	0.476	0.470
u-b	---	---	1.230:	1.254:	1.227:	1.256:	1.335
b-y	-0.010	-0.022	-0.027	-0.025	-0.009	-0.022	-0.004
Δa	0.012	0.017	0.018	0.020	0.021	0.021	0.024
Δa'	0.038	0.049	0.058	0.066	0.054	0.064	0.057
Δ_1**	0.032:	0.034:	0.022	0.018	0.016	0.021	0.017

λ(Å)	8	9	10	Average
3300	1.159	1.176	1.190	1.175
3390	1.156	1.160	1.195	1.175
3448	1.129	1.141	1.163	1.147
3509	1.084	1.095	1.116	1.103
3571	1.080	1.089	1.108	1.080
3636	1.040	1.055	1.073	1.043
3704	1.005	1.009	1.025	1.013
4032	-0.128	-0.143	-0.132	-0.138
4167	-0.094	-0.102	-0.093	-0.102
4200	-0.088	-0.099	-0.087	-0.091
4255	-0.095	-0.101	-0.086	-0.099
4464	-0.166	-0.117	-0.099	-0.119
4566	-0.069	-0.084	-0.069	-0.080
4785	-0.074	-0.070	-0.059	-0.072
5000	0.000	0.000	0.000	0.000
5128	0.038	0.033	0.034	0.035
5200	0.085	0.083	0.086	0.085
5264	0.082	0.086	0.096	0.084
5360	0.086	0.086	0.087	0.086
5470	0.090	0.087	0.090	0.089
5556	0.096	0.106	0.099	0.099
5840	0.114	0.133	0.121	0.126
6020	0.167	0.174	0.166	0.169
6058	---	---	---	0.171
6220	0.194	0.216	0.218	0.209
6370	0.220	0.221	0.214	0.224
6650	0.265	0.276	0.272	0.271
6800	0.278	0.298	0.284	0.289
7100	0.317	0.343	0.325	0.337
7530	---	---	---	0.425
7850	---	---	---	0.464
u-b	1.312	1.329	1.336	1.330
b-y	-0.006	-0.015	-0.002	-0.012
Δa	0.028	0.028	0.031	0.028
Δa'	0.062	0.050	0.059	0.051
Δ_1	0.013	0.014	0.012	0.015
Δ_1*	0.037	0.038	0.030	0.042
Δ_1**	0.021	0.025	0.022	0.025

TABLE AI. — *Relation of index and b-y ; of form* $x_0 = a + b(b-y) + c(b-y)^2$.

x_0	a	b	c	Grid	Scatter (rms)	Criteria for Presence Marginal	Definite
a_0	0.0009	0.0538	0.0000	1	0.003	0.009-0.012	>0.013
a_0	0.0018	0.0510	0.0000	2	0.004	0.009-0.012	>0.013
a_0'	0.0124	0.1764	0.0000	1	0.005	0.010-0.012	>0.013
a_0'	0.0164	0.1271	0.0000	2	0.007	0.010-0.012	>0.013
l_0	0.0075	0.0240	-0.3201	2	0.007	0.014-0.016	>0.017
l_0*	-0.0039	0.2802	-0.6468	2	0.009	0.012-0.020	>0.021
l_0**	0.0087	0.1401	-0.7578	2	0.010	0.015-0.020	>0.021
l_0**	0.0089	0.0522	-1.8457	1	0.005	0.015-0.020	>0.021

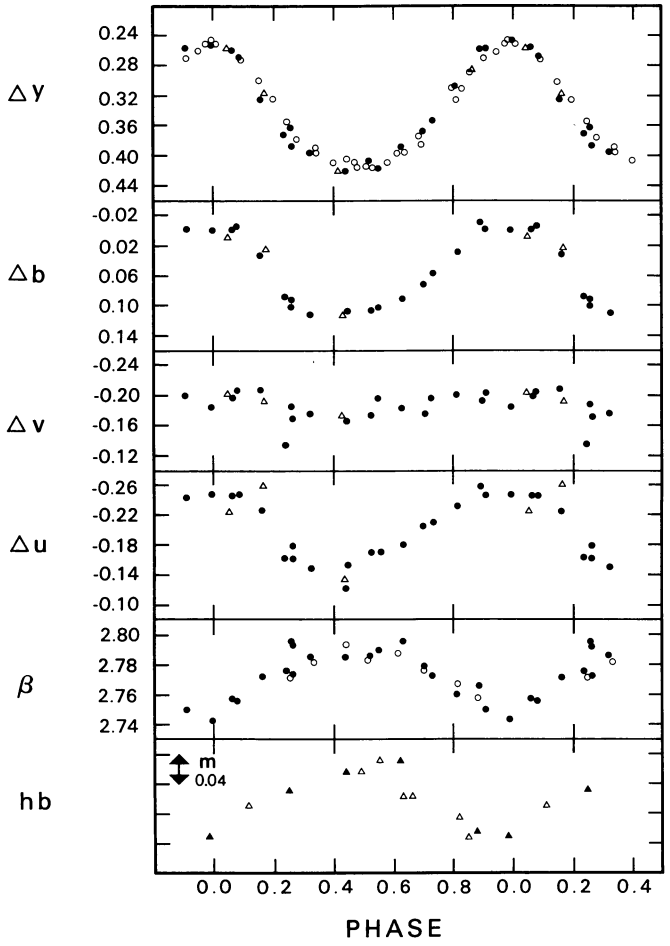

FIGURE 1. — Photometric variations with phase of HD 51418. In all except the bottom two plots, all values are relative to the comparison star 60 Aur. The four-color photometry of D. M. P. is represented by closed circles in all plots. In the top plot the open circles represent the Δv values of Gulliver and Winzer (1973), with an arbitrary shift in magnitude. In the β *vs.* phase plot, the open circles are the β values of Gulliver and Winzer. The open triangles represent the following spectrophotometric values (with an arbitrary magnitude shift) : $\Delta m(5556)$, $\Delta m(4566)$, $\Delta m(4167)$ and $\Delta m(3509)$, in the Δy, Δb, Δv and Δu plots, respectively. In the bottom plot, the closed triangles represent the *hb* values (defined in the text) for scans 5-9 and the open triangles, for scans 10-15. They are shifted by an arbitrary amount in magnitude to account for the different bandpasses used.

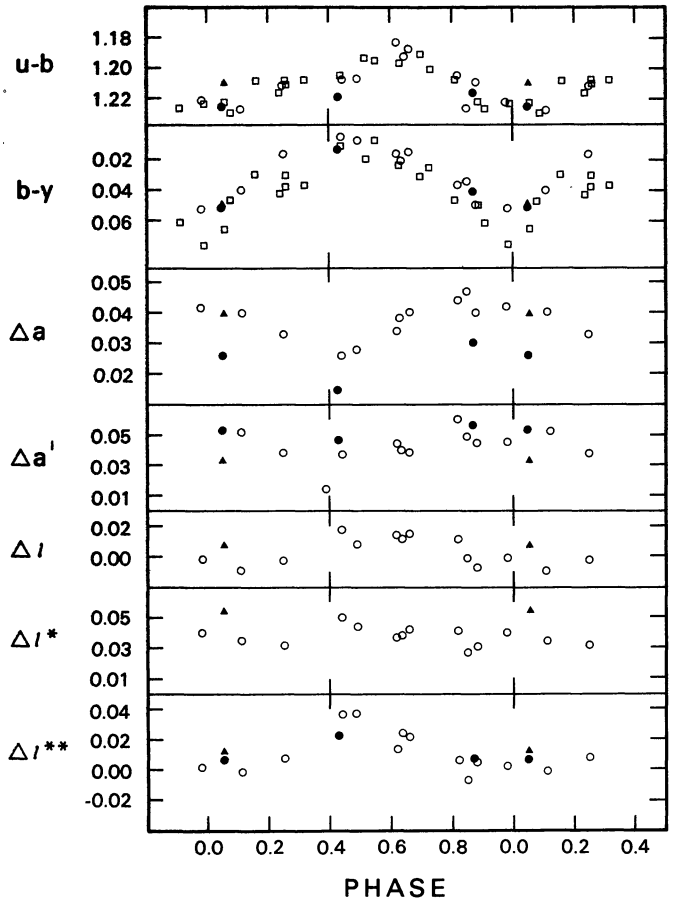

FIGURE 2. — The index values of HD 51418 as a function of phase. Closed circles are scans 1-3, closed triangle, scan 4 and open circles, scans 5-15. The four-color *u-b* and *b-y* values of D. M. P. are represented by open squares.

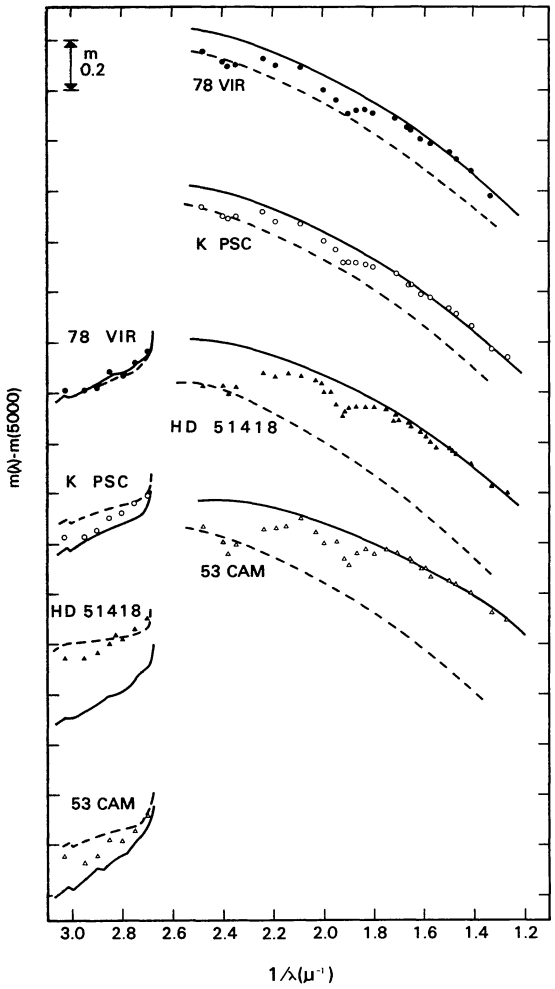

FIGURE 3. — The observed average energy distributions, normalized to λ 5000, of four Ap stars; 78 Vir (closed circles), κ Psc (open circles), HD 51418 (closed triangles) and 53 Cam (open triangles), compared with solar composition, log g = 4.0 model atmospheres that best match the Paschen continuum (solid lines) and the Balmer jump (dashed lines). The predictions of the models in the region of the Balmer confluence are not shown. The effective temperatures of the models are : 78 Vir, BJ, 10000 K and PC, 9500 K ; κ Psc, BJ, 10250 K and PC, 9500 K ; HD 51418, BJ, 11500 K and PC, 9000 K ; and 53 Cam, BJ, 10250 K and PC, 8500 K.

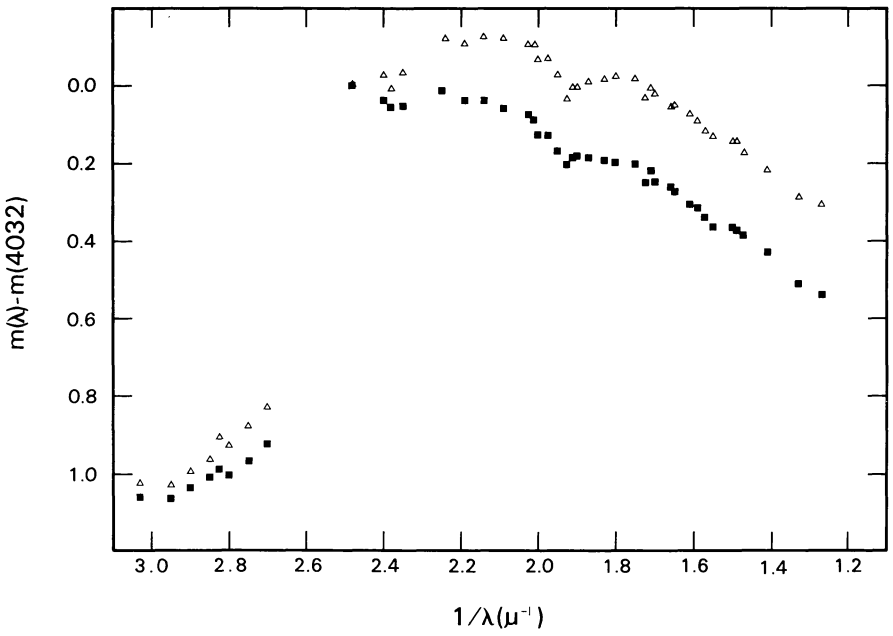

FIGURE 4. — Energy distributions of HD 51418, normalized to λ 4032, at the phases of their maximum difference in *b-y* and *u-b*. Open triangles represent the reddest colors at $\phi \cong 0.0$ (average of scans 2, 4 and 9); closed squares represent the bluest colors at $\phi \cong 0.45$ (average of scans 3, 7 and 12).

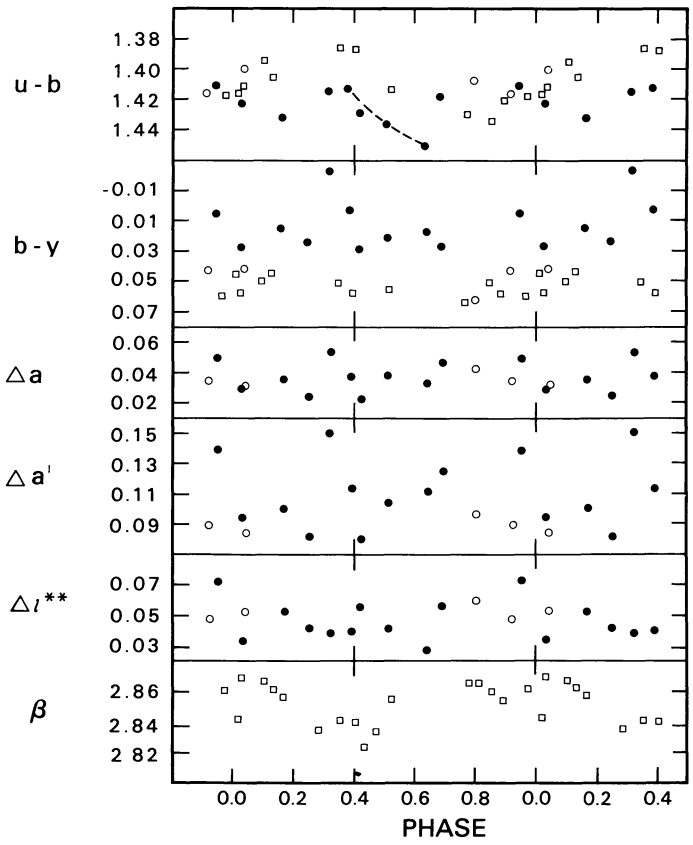

FIGURE 5. — The index values of 53 Cam as a function of phase. Closed circles represent the spectrophotometric values of D. M. P., open circles those of S. J. A. and open squares the four-color photometry of D. M. P. The three points connected by a dashed line are discussed in the text.

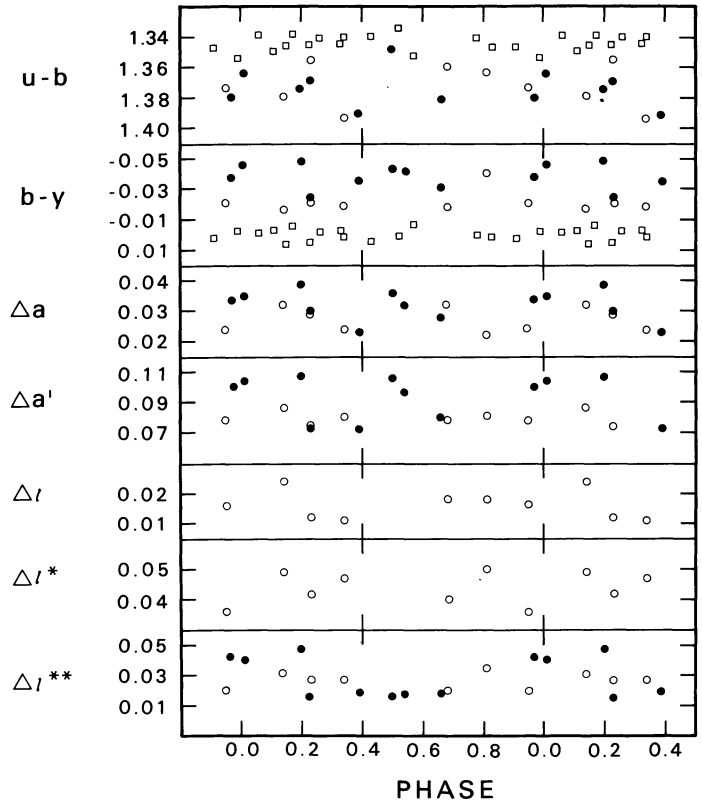

FIGURE 6. — The index values of 78 Vir as a function of phase. Symbols are the same as in figure 5, except the open squares in the *u-b* and *b-y* plots represent the four-color photometry of Wolff and Wolff (1971).

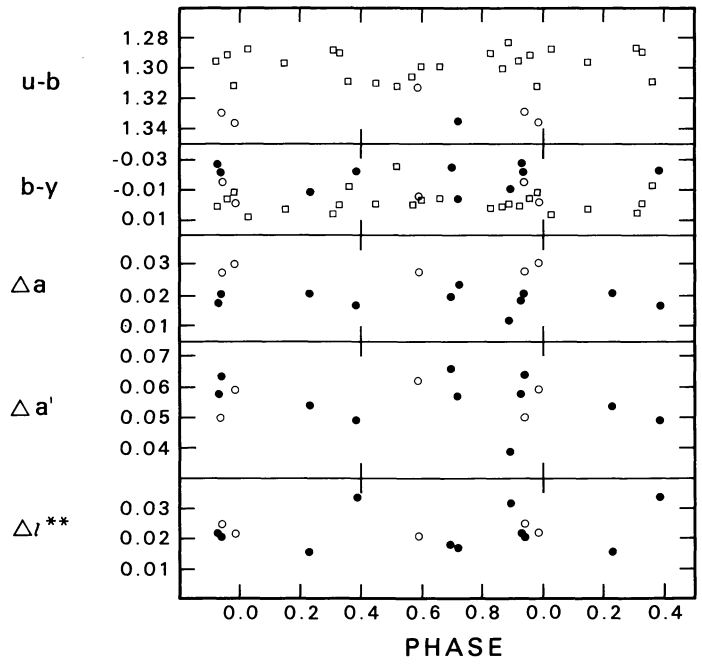

FIGURE 7. — The index values of κ Psc as a function of phase. Symbols are the same as in figure 5.

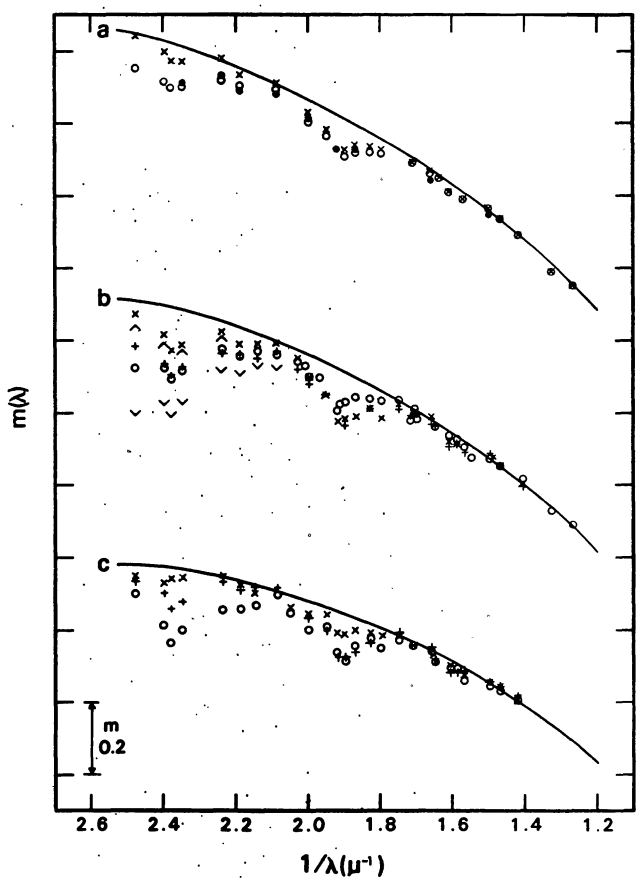

FIGURE 8. — Comparison of the energy distributions in the Paschen continuum of Ap stars with the predictions of solar composition, log $g = 4.0$ model atmospheres. *a*. The solid line represents a 9500 K model. HD 111133 (Adelman, 1981a) and the averages of 78 Vir and κ Psc are represented by crosses, open circles and closed circles, respectively. Where the values for κ Psc and 78 Vir coincide, only an open circle is drawn. *b*. The solid line represents a 9000 K model. HD 50169 and HD 110066 (Adelman, 1981b) are represented by crosses and plusses, respectively; the average of HD 51418 by open circles. The brackets indicate the extremes of the values for HD 51418 in the shortward end of the Paschen continuum; the top bracket represents $\phi = 0.5$ and the bottom bracket $\phi = 0.0$. No bracket is drawn where the top bracket coincides with a cross. *c*. The solid line represents a 8500 K model. HD 204411 (Adelman, 1981c), HD 2453 (Adelman, 1981b) and the average of 53 Cam are represented by crosses, plusses and open circles, respectively.